Polymer 212 (2021) 123309

Contents lists available at ScienceDirect

Polymer

journal homepage: http://www.elsevier.com/locate/polymer

Unusual low temperature relaxation behavior of crosslinked acrylonitrile-butadiene co-polymer

Debdipta Basu [a,*], Shib Shankar Banerjee [b], Subhas Chandra Debnath [c], Mikhail Malanin [b], Lyaysan Amirova [e], Philippe Dubois [g], Gert Heinrich [b,f], Amit Das [b,d]

[a] Indian Rubber Manufacturers Research Association, Thane (W), 400604, India
[b] Leibniz-Institut für Polymerforschung Dresden e.V., Dresden, 01069, Germany
[c] Department of Chemistry, University of Kalyani, Nadia, 741235, West Bengal, India
[d] Tampere University of Technology, Department of Materials Science, P.O. Box 589, FI-33101, Tampere, Finland
[e] University of Applied Science, Northwestern Switzerland, Klosterzelgstrasse 2, 5210, Windisch, Switzerland
[f] Technische Universität Dresden, Institute of Textile Machinery and High Performance Material Technology, Dresden, 01069, Germany
[g] Center of Innovation and Research in Materials & Polymers – CIRMAP Laboratory of Polymeric and Composite Materials, University of Mons, Belgium

ARTICLE INFO

Keywords:
Nitrile rubber
Zinc chloride
Coordination complex in elastomer
Low temperature relaxation dynamics
Metathesis

ABSTRACT

Conventional crosslinking of rubbers (using sulphur and peroxide vulcanization) usually leads to covalent rubber network junctions. The present article reports about a new unconventional crosslinking of acrylonitrile butadiene copolymer (NBR) by zinc chloride ($ZnCl_2$). This crosslinked NBR displayed very interesting relaxation properties below the glass transition temperature. In this work, detailed chemical mechanistic pathways were suggested and correlated with the low-temperature relaxation dynamics of the crosslinked material. Fourier-transform infrared spectroscopy analysis clearly indicated a coordination effect between zinc and nitrile groups. At lower temperatures, beside the glass transition, another relaxation process (β relaxation) was detected. Interestingly, a hydrolyzed crosslinked sample showed even two other additional relaxation processes. The origin of such relaxations was critically discussed from the viewpoints of modification of the polymer chains as well as low molecular weight fragments of the polymer.

1. Introduction

Crosslinking or vulcanization of rubber is a topic of study since many years. Currently, sulphur and peroxide crosslinking are main industrial techniques for curing of various rubbers. Intensive analysis was done to understand the inherent mechanisms of such types of crosslinking processes over the decades [1–5]. These methods lead to chemical crosslinks, however they prevent melt reprocessing and recycling which are essential to re-usage of waste vulcanized rubber as a material for environment conservation and thermal energy source [6]. Therefore, the efforts grow worldwide to develop a rubber recycle method of crosslinked rubbers for environmental conservation, which is undoubtedly a big challenge in rubber technology today. Reversible crosslinking of rubbers, in such instances, can be an alternate to solve the issue of environmental conservation and energy sources. Reversible crosslinking generally originated and associated from different chemical interactions such as ionic interaction, hydrogen bonding and crystallinity in polymeric systems [7–10]. Additionally, a few other types of crosslinking processes, for example metal oxide induced crosslinking [10–13], co-ordination network [14], electron induced reactive processing [15–17] etc. were also used to some extent with some specific rubbers and thermoplastic elastomers. These types of crosslinking techniques are non-conventional. In addition, the development of rubbery materials using non-conventional crosslinking is the current research interest. The present article explores a non-conventional crosslinking of acrylonitrile butadiene rubber in presence of metal salt like $ZnCl_2$. Till date, there are limited reports concerning studies and discussion on the metal ions induced network formation of different rubbers [18–22]. Some recent reports [23,24] can be found on metal coordination network of elastomers, but neither of them evinced and subsequently established the nature of the central metal ion-based co-ordination. Availability of more than one functional moiety in the NBR offers ample scope to interact with $ZnCl_2$. Simultaneous presence of the acrylonitrile groups and the unsaturation in the backbone structure

* Corresponding author.
E-mail address: db@irmra.org (D. Basu).

https://doi.org/10.1016/j.polymer.2020.123309
Received 2 October 2020; Received in revised form 27 November 2020; Accepted 5 December 2020
Available online 9 December 2020
0032-3861/

generally yields two different types of vulcanization reactions while treated with a variety of transitional metal ions like Zn^{2+}, $Cu^{2+,}$ etc. [11]. The complex structure generated by such types of reactions provides an essential chemical heterogeneity to the system [11].

In this current study, several characterization techniques for example dynamic mechanical analysis, tensile testing, differential scanning calorimetry, Infrared spectroscopy (FTIR), Scanning Electron Microscopy (SEM) associated with Energy Dispersive X-ray Spectroscopy (EDX) were employed to understand different chemical microstructures formed during the crosslinking process. Experimental evidences were provided for the evolution of new kind of main chain modification and associated mechanical properties of the material.

2. Experimental section

2.1. Materials

Acrylonitrile butadiene rubber (NBR) was kindly supplied by Lanxess (Leverkusen, Germany). In this work, five different grades of NBR were used depending on the acrylonitrile content and Mooney viscosity. N18, N26, N33, N44 and N49 indicate NBR rubbers with 18, 26, 33, 44 and 49 wt% of acrylonitrile contents, respectively. High cis-polybutadiene (Buna CB 24) used in the study was also collected from Lanxess (Leverkusen, Germany). $ZnCl_2$ (purity ~ 99%) and Mercaptobenzothiazole disulfide (MBTS) was purchased from Acros Organics. Formulation of $ZnCl_2$ and Sulphur based NBR samples are given in Table 1.

2.2. Compounding and preparation of crosslinked rubber

All the rubber composite samples were prepared using a two-roll mixing mill (Polymix 110L, size: 203 × 102 mm^2, Servitech GmbH, Wustermark, Germany) with a friction ratio of 1:1.2, at 40 °C using a 15 min compounding cycle. All weights were taken in phr (parts per hundred of rubber). After the compounding steps, the samples, thus obtained, were subjected to a curing study to determine the optimum curing time. In this procedure, an uncured mass (~5.5 g) from the compounded rubber was kept in a rubber process analyzer (RPA) (Scraeabaus SIS–V50) under isothermal conditions at 160 °C with a frequency of 1.67 Hz, and the torque value was plotted against time. From this torque-time curve, the optimum curing time (t_{90}), defined by the time to reach 90% of its ultimate rheometric torque value was estimated.

All values are in parts per hundred parts of rubber (phr)

The rubber samples were then cured for this optimal amount of curing time (t_{90}) by a hot press (FORTUNE Holland, Model TP 400) at 160 °C, cooled to room temperature and then kept for 24 h before performing any further characterization. The activation energy for the curing reaction was determined from Arrhenius method. The rate constants of the crosslinking reaction were evaluated by the following autocatalytic kinetic model which can be written as

$$\frac{da}{dt} = k(T)a^m(1-a)^n \tag{1}$$

where k is the temperature dependent rate constant, m and n are the orders of reactions, which also depend on reaction temperature. Here, the extent of the cure at the time t can be expressed as

$$a\frac{M_t - M_0}{M_h - M_0}. \tag{2}$$

where Mt is the torque value at the time t, Mh is the highest torque within the experimental time, M0 is the lowest rheometric torque value. The values of k, m and n are estimated using non-linear multiple regression analysis of the experimental data. The function $k(T)$ can be expressed by the Arrhenius equation.

$$k = Ae^{-Ea/RT} \tag{3}$$

where A is the pre-factor and E_a is the activation energy.

3. Characterization

3.1. Fourier transform infrared spectroscopy (FTIR)

To obtain FTIR-spectra of NBR-based specimens in order to characterize samples chemically, an evacuated FTIR spectrometer Vertex 80v (Bruker) equipped with attenuated total reflection unit (ATR-Golden Gate unit, SPECAC) und liquid nitrogen cooled detector (Bruker) were used. The spectra were measured in spectroscopic range 4000-600 cm^{-1}. Every spectrum was averaged over 100 scans. To compare spectral data properly the baseline correction, subtraction of diamond (ATR-crystal) bands as well as spectra's normalization (using asymmetrical stretching vibration band of methylene group at 2919 cm^{-1} as an internal reference [25,26]) was applied.

3.2. Tensile tests

Tensile tests of the NBR vulcanizates were done using a Zwick 1456 (model 1456, Z010; Ulm, Germany) with crosshead speed of 200 mm min^{-1} in accordance with ISO 527:2012.

3.3. Swelling study (crosslink density measurement)

To analyze the network structure of the $ZnCl_2$ cured NBR compounds, swelling test was carried out based on the ASTM D6814−02 standard. According to this standard, specimens were swollen in a solvent with the knowledge of the polymer - solvent interaction parameter. Toluene was used here as solvent. The swelling phenomenon is not explored with other solvent except toluene due to limited scope of the study and deep understanding of the crosslinking mechanism of such a complex system influenced by single solvent. In near future, we will continue this study with a set of polar solvents and toluene to explore more insight of crosslink density and complex break down. Pre-weighed rubber specimens were swollen for 24 h at room temperature. The solvent was replaced with fresh solvent from time to time during this test. After swelling, the solvent was wiped off quickly from the surface of the specimens using a clean blotting paper. The samples then were dried at 70 ± 2 °C in a forced-ventilating air oven for around 16 ± 1 h until constant weight. The samples were next allowed to cool down to room temperature using a desiccator and weights were taken. The volume fraction of rubber in the swollen gel () were calculated from the following equation which is based on the simple additive rule of volumes

Table 1
Formulation of the rubber compounds.

Ingredients	N_{18}	N_{26}	N_{33}	N_{44}	N_{49}	$N_{18}S$	$N_{26}S$	$N_{33}S$	$N_{44}S$	$N_{49}S$
NBR	100	100	100	100	100	100	100	100	100	100
$ZnCl_2$	20	20	20	20	20	–	–	–	–	–
ZnO	–	–	–	–	–	5	5	5	5	5
Stearic acid	–	–	–	–	–	2	2	2	2	2
Sulphur	–	–	–	–	–	1	1	1	1	1
MBTS	–	–	–	–	–	2	2	2	2	2

as follows:

$$V_r = \frac{(D - FH)/\rho_r}{(D - FH)/\rho + A_0/\rho_s} \quad (4)$$

where H = initial weight of the test specimen, = deswollen weight of the test specimen (until constant weight), F = weight fraction of the insoluble components, such as fillers, = weight of the absorbed solvent (= immediate weight –), ρ_r = density of the rubber, ρ_s = density of the solvent.

At swelling equilibrium condition the classical Flory-Rehner [27] equation was given by:

$$-\left[\ln(1 - V_r) + V_r + \chi V_r^2\right] = \frac{\rho_r}{M_C} V_s \left(1 - \frac{2}{f}\right) V_r^{1/3} \quad (5)$$

where f is crosslinking functionality, is the Flory-Huggins polymer-solvent interaction parameter.

If the crosslinking functionality was considered to be tetra-functional ($f = 4$), then the apparent crosslinking density (ν_c) can be expressed in the following equation:

$$\mathrm{VC} = 12\mathrm{MC} = -\ln(1 - \mathrm{Vr}) + \mathrm{Vr} + \mathrm{XVr2VSVr.3Vr1/32} \quad (6)$$

where V_r is the volume fraction of the polymer in the swollen specimen, is the Flory-Huggins polymer-solvent interaction parameter (0.3795 for NBR-Toluene system) [28], is the (average) molecular weight between two crosslinks, and V_S is the molar volume of the solvent. Considering the chemical structure of a zinc nitrile complex with four network chain paths connecting this complex with four topologically neighbouring complexes, we assume a tetra-functional ($f = 4$) crosslinking functionality as demonstrated in Fig. 1b.

3.4. Dynamic mechanical analysis (DMA)

Dynamic mechanical properties were measured using a dynamic mechanic thermic spectrometer, DMTS (GABO Eplexor 150N) in tension mode. All the samples (length 35 mm, width 10 mm, thickness 2 mm) were analyzed at a constant frequency of 10 Hz, at a heating rate of 2 K/min and a pre-strain of 0.5% over a temperature range of −150 °C to +100 °C. Storage modulus (E′), loss modulus (E″) and loss factor (tanδ) were measured as a function of temperature.

3.5. Field emission scanning electron microscopy (FESEM)

The phase morphology of the samples was recorded from FESEM (Zeiss Ultra Plus, Carl Zeiss Microscopy GmbH, Jena, Germany) equipped with an energy-dispersive X-ray spectrometer (EDX; Quad XFlash 5060, Bruker Corporation, Billerica, MA). Rubber specimens were cut into small square shapes. Prior to the experiment, all the rubber specimens were gold sputtered for 30 s to avoid charging on exposure to electron beam during FESEM analysis.

3.6. Differential scanning calorimetry (DSC)

DSC study was carried out for all the samples using Q1000, TA Instruments, USA coupled with an auto-sampler in the temperature range of −160 °C–100 °C in nitrogen atmosphere at the heating rate of 10K/min. Low temperature DSC analysis was also performed in the range of −175 °C–100 °C with a heating rate of 10K/min.

4. Results and discussion

The rheometric studies are witnessed for 1 h. During this tenure, all the curves show marching type of curing and the optimum curing time is challenging to be obtained from the experimental curing data. Therefore, the optimum curing time (t90) was calculated by considering 1 h rheometric data.Crosslinking of NBR in presence of $ZnCl_2$ was first investigated from rheometric study (Fig. 1a). NBR based rubber compounds with varying acrylonitrile (-CN) content were prepared by mixing with 20 phr of $ZnCl_2$.

The curing of NBR by $ZnCl_2$ could be explained by different chemical pathways. The first mechanism could be related to the formation of coordination bond (Fig. 1c) formation between the nitrile groups [24]. Other possibilities were covalent crosslinking in two different mechanisms; one was $ZnCl_2$ assisted carbocationic path (Fig. 2) [29] and another one was participation of the different nitrile groups in imine bond formation (Fig. 3) [30]. It could be seen from rheometric study

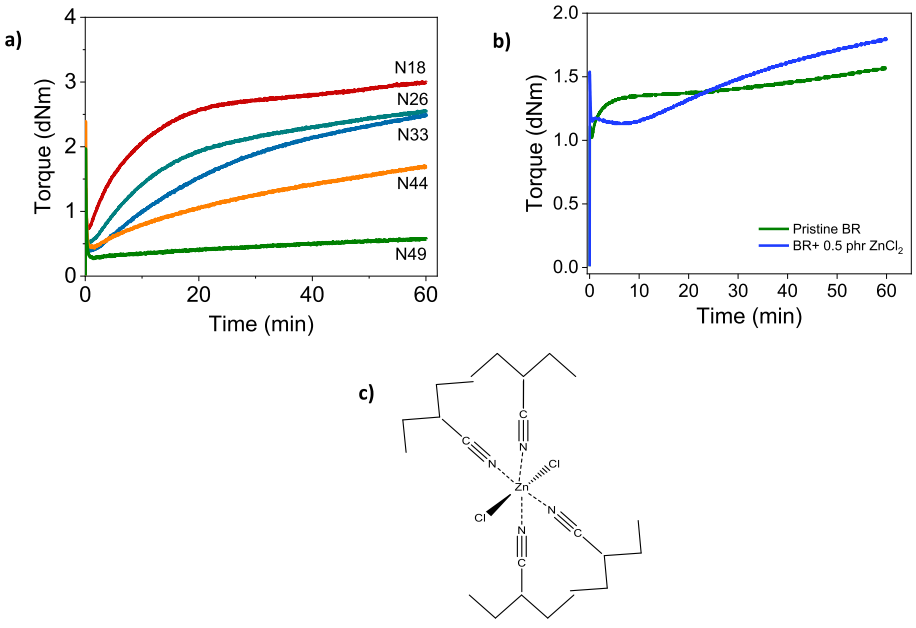

Fig. 1. a) Rheometric characterization for the curing of NBR compounds comprised with $ZnCl_2$. NBR used here contained different quantities of nitrile contents and the studies were carried out at 160 °C for 1 h, b) development of rheometric torque of polybutadiene rubber in presence of very small amount of zinc chloride (0.5 phr) at 160 °C temperature, c) the chemical structure of zinc nitrile complex resulting polymer network.

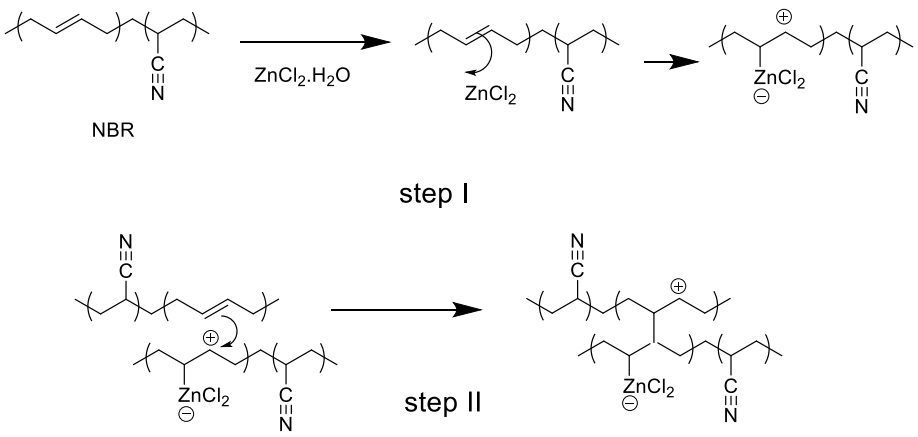

Fig. 2. Schematic presentation of cationic crosslinking reaction assisted by $ZnCl_2$. In step I a carbocation is formed and in the step II the carbocation is promoting crosslinking reaction with double bond.

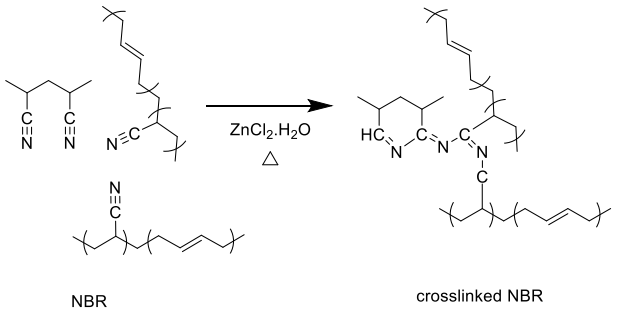

Fig. 3. Schematic presentation of network formation with participation of several nitrile group of random co-polymer of acrylonitrile and butadiene. The reaction is facilitated by zinc-nitrile complex (Fig. 1b).

(Fig. 1a) that N18 (-CN ~ 18%) yielded the highest dynamic modulus (~2.8 MPa) despite the fact that it had the lowest amount of acrylonitrile content compared to the other compositions. Increased amount of acrylonitrile content and subsequently gradual decrease of butadiene group present in the host rubber resulted in lower modulus for the vulcanizates indicating lower crosslinking densities of the respective samples. As obvious from the Fig. 1a, the torque development is almost negligible for N49 even after 1 h curing. However, after compression molding, the material was found to be defective, degradative mash. The higher modulus value at lower nitrile content could be corroborated to the probability of higher crosslinking extent associated with unsaturation of butadiene unit. In this study, the probable chemical mechanisms were envisaged to understand the crosslinking process associated with $ZnCl_2$ and nitrile group (Figss. 1–3) [29–31]. Comparatively few published information related to the chemical interaction between polyacrylonitrile and $ZnCl_2$ in nitrile butadiene rubber compounds offered limited scope to exploit the mechanism. Nevertheless, Zil'berman et al. [30] explored the influence of different chemical sources like water, alcohols, carboxylic acids, hydrogen sulphide etc. with nitrile rubber and $ZnCl_2$ to comprehensively understand the indicative mechanism with scientific conviction. The crosslinking mechanism related with double bonds might be involved with carbocation type polymerization [32] which was still not confirmed but somehow could be explained as shown in Fig. 2. Two stage cross-linking mechanism was proposed between NBR and $ZnCl_2$. In the first step, as nitrile rubber reacted with $ZnCl_2$, carbocation formed on elastomer chain. Crosslinking of acrylonitrile butadiene rubber does not take place in absence of $ZnCl_2$. Moreover, presence of nitrile group is not essential since similar reaction occurs with butadiene rubber. In Fig. 1b the rheometric characterisation of pure butadiene rubber (BR) mixed with very small amount of zinc chloride (0.5 phr) is shown which is measured at 160 °C. For comparison, raw butadiene rubber also tested at similar condition to check only thermal crosslinking reaction. Though the development of torque with zinc chloride is not that much pronounced but rise in torque value indicates that zinc ion acts as Lewis acid and chemically participates in the crosslinking process which is taking place by the active involvement by the double bonds present in BR. Therefore, crucial role of $ZnCl_2$ as a crosslinker is very much evident. It appears that $ZnCl_2$, being a π-electrophilic Lewis acid, could polarize the π-bond present in the NBR back bone. This $ZnCl_2$ assisted activation of π-bond leads to formation of a highly reactive carbocation intermediate which is susceptible to nucleophilic attack by the neighbouring π-bond of NBR chain. This is how C–C fusion of two olefin moiety takes place with simultaneous generation of another reactive carbocation intermediate to continue the crosslinking via chain reaction. In the second step, the highly reactive carbocation formed interacted with the butadiene segment and eventually leaded to cross-linking of the neighbouring rubber chain. Similar mechanism was reported by Desai et al. [29] while studying with polychloroprene rubber and $ZnCl_2$. It is noteworthy to state that, this kind of reaction mechanism is merely speculative and till date there is no direct evidence to support. Therefore, there is a dire need to establish some reaction pathways based on organic chemistry reaction principle. This indeed helps to unravel the crosslinking reaction and the complex nature of the network structure of similar nature as of the discussed system. Fig. 3 demonstrated the stipulated mechanism on how network formation took place during crosslinking in NBR-$ZnCl_2$ system. The crosslinking between the random copolymer of NBR under the influence of $ZnCl_2$ took place relying on nucleophilic reactivity of the nitrile group leading to imide linkage [30].

Possible multiple mechanical relaxation phenomena have been studied in a crosslinked sample and to understand the origin of each relaxation is the major concern of this study. Unfortunately, due to the crosslinked nature of the sample, it is extremely challenging and difficult to extract the information by segregating the part of the modified portions of the macromolecular chain. In order to understand the crosslinking kinetics in this system, a conventional sulphur based formulation was also considered and compared. The network formation by sulphur based conventional ingredients and with $ZnCl_2$ were taking place via different chemical mechanisms which were reflected in the cure kinetics (Fig. 4). The activation energies were found to be 72 and 61 kJ mol^{-1} for $ZnCl_2$ and sulphur based compounds, respectively.

The interaction between NBR and $ZnCl_2$ was studied by FTIR-spectroscopy. Fig. 5 presented a typical ATR-FTIR spectrum of different NBR samples. As it was unambiguously demonstrated, the incorporation of $ZnCl_2$ brought considerable amount of water into NBR-system what was confirmed by presence of new specific broad water

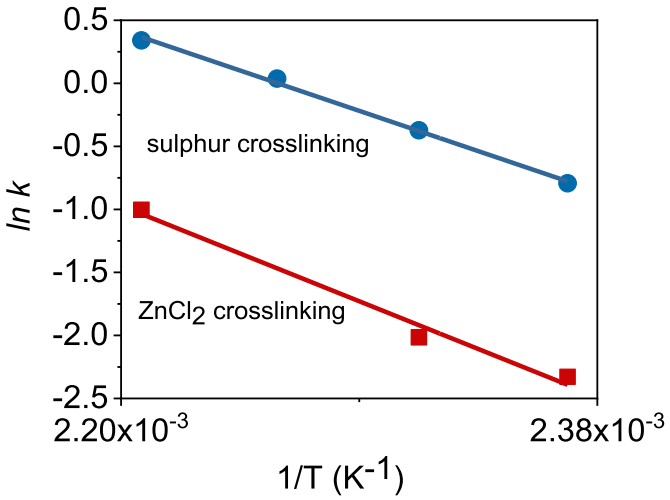

Fig. 4. Arrhenius type plot of ln K versus 1/T for the calculation of the activation energy for NBR with $ZnCl_2$ and conventional sulphur based recipe *(ZnO-5 phr, stearic acid-2 phr, MBTS-2 phr and sulphur-1 phr).*

bands at 3428, 1638 and around 690 cm^{-1} [26] in comparison with the spectrum of initial NBR-sample (neat). This effect was completely expected, because $ZnCl_2$ was known to be very hygroscopic. Additionally, a new band at 2261 cm^{-1} reflected a coordination effect between zinc and nitrile group [24]. The evaluation of several chemical groups by the reaction of NBR and $ZnCl_2$ were demonstrated in Fig. 6.

Surprisingly, the spectrum of neat NBR showed bands of medium intensity at 1538 cm^{-1} and about 1400 cm^{-1} (as a shoulder) what was typical characteristic for triazine group as schematically displayed in Fig. 6 [26,31–33]. Probably, the triazine functionality could be formed courtesy to the availability of three adjacent nitrile groups [29] at the close vicinity. So, this triazine formation can also take place at room temperature during storage of the commercial materials. Incorporation of $ZnCl_2$ might initiate the opening of triazine ring (Fig. 6) and this could be the reason for band's intensity decrease [33] with simultaneous increase of nitrile band at 2237 cm^{-1} (see inset in Fig. 5).

The effect of hydrolysis on the NBR samples was also analyzed. The spectrum of hydrolyzed samples showed a slight increase of water bands (Fig. 5) as well as further decay of triazine bands mentioned above and at the same time the coordination band of nitrile group with zinc at 2261 cm^{-1} almost disappeared (see inset in Fig. 5). Lower coordination of nitrile groups after hydrolysis was quite expected, because $ZnCl_2$ was water-soluble and was washed out from the rubber system. Probable rubber degradation (e.g. hydrolysis of nitrile group into amide and carboxylic functionalities) was disguised by aforementioned effects and by broad water bands in this case, because these processes were parallel and it explained the absence of further intensity changes of nitrile band in the spectra. It could be mentioned here that the carboxylic group produced from the hydrolysis of the nitrile group could undergo further crosslinking reaction with the double bond present in the rubber chain [21,22].

The existence of the peak at 686 cm^{-1} was may be due to the water present caused by the incorporation of zinc chloride into the system. Two weak bands of NBR compound with $ZnCl_2$ after Hydrolysis were obtained at 1770 and 1830 cm^{-1}, what can be of carboxylic acid chloride (only for 1770 cm^{-1}) and carboxylic acid anhydrides (C═O stretching) vibrations and simultaneously C═O band of isolated carboxylic groups respectively [33–35]. Therefore, those two peaks at 1770 cm^{-1} to 1830 cm^{-1} attributed to the cross-linking of the macromolecules largely due to the intermolecular addition of the carboxylic acid anhydrides formed in the hydrolysis with the C═C double bonds which eventually resulted to enhanced crosslinking degree [Fig. 6] [21,22]. Ammonia liberated during this process catalyzed the corresponding reactions and the direct hydration of the acrylonitrile groups to amide groups following the schematic presentation as shown in Fig. 6 [33]. The crosslinking of the macromolecules was corroborated to a significant degree to the intermolecular addition of the carboxyl groups formed in the hydrolysis to the C═C double which subsequently produced ester groups as schematically exhibited in Fig. 6 [30].

In order to gain a deep insight to understand the crosslinking

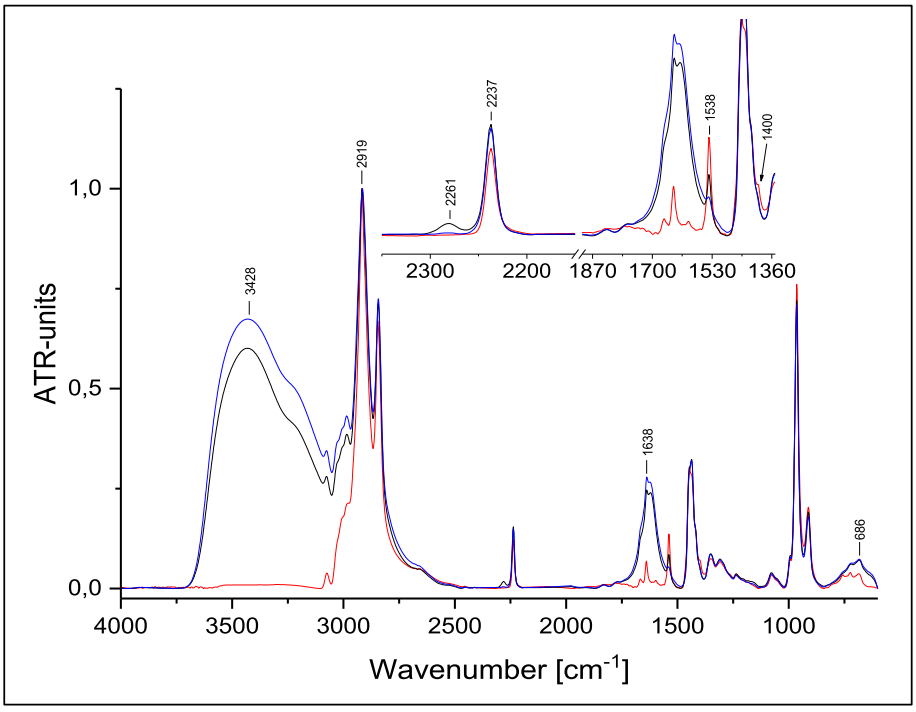

Fig. 5. ATR-FTIR spectra of neat (red), NBR compound with $ZnCl_2$ (black) and hydrolyzed modified with $ZnCl_2$ (blue) NBR-samples (the magnified region from 2400 to 1360 cm^{-1} is exhibited at the inset). (For interpretation of the references to colour in this figure legend, the reader is referred to the Web version of this article.)

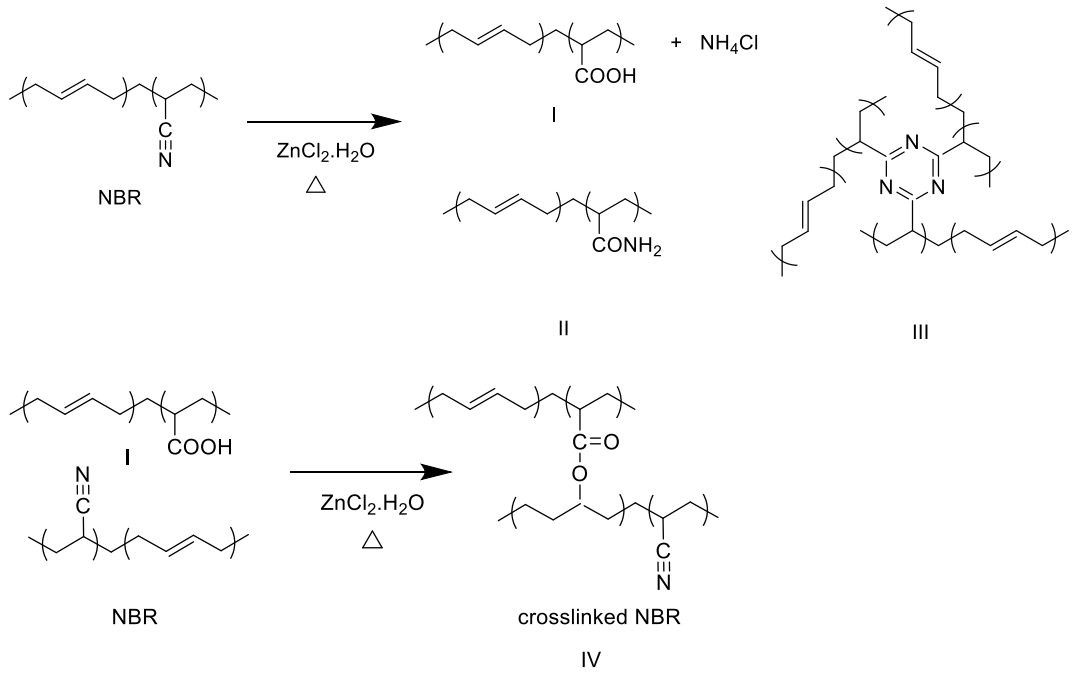

Fig. 6. Schematic presentation of the reaction products when acrylonitrile butadiene copolymer is allowed to reaction with $ZnCl_2$ at 160 °C temperature, I) transformation of nitrile group into acid, II) acetamide, III) triazine crosslinking, and IV) ester crosslinking by the reaction of produced acid and double bond of the butadiene unit.

behavior of the NBR, crosslink density was estimated by equilibrium swelling method as well as using Mooney-Rivlin (MR) equation as summarized in Table 2. Both the experimental values and fitting curve obtained values are close to each other (Table 2).

The corresponding Mooney-Rivlin (MR) plot is shown in Fig. 7a. For MR studies, a plot of reduced stress versus stretching ratio was presented and the slope and the intercept [36,38] obtained by fitting a straight line were taken into consideration to calculate the crosslink density.

$$\text{Reduced stress.} = \frac{\sigma}{2(\lambda - 1/\lambda^2)} \tag{7}$$

$$\frac{\sigma}{2(\lambda - 1/\lambda^2)} = c_1 + c_2 \Big/ \lambda \tag{8}$$

$$\text{Crosslink density} = \frac{1}{M_c} = c_1/RT \tag{9}$$

where, σ = stress of the samples measured by classical stress-strain experiment obtained from Fig. 7b, λ = stretching ratio, c_1 = intercept of the MR plot, c_2 = slope of the MR plot, crosslink density expressed by the reciprocal of the molecular weight between two successive crosslinks (M_c) [11,36,37], R = universal gas constant (8.314 J K^{-1} mol^{-1}) and T is the ambient temperature (298 K). It needed to be mentioned here that the values of c_1 was found to be the highest and c_2 the lowest in case of lower acrylonitrile content NBR. In addition, the crosslink density values were found to be the highest in case of the N18 sample with lower acrylonitrile content in both the cases. This observation was in accord with the rheometric behavior of the compounds as discussed earlier. It was observed that N18 sample offered higher crosslink density value which was estimated from Mooney-Rivlin plot and could be nicely correlated with the classical stress strain data obtained in Fig. 7b. N18 displayed the highest modulus at 200% elongation (2.32 MPa) compared to other vulcanizates like N26 (1.15 MPa), N33 (1.38 MPa) and N44 (1.69 MPa). The tensile strength of N18 sample was found to be the highest (3.7 MPa) and elongation at break was 252%, however, the N26 and N33 samples showed almost same and highest elongation at break (435%) as compared with other samples.

Table 2
Crosslink density values calculated for NBR vulcanizates[a] by swelling and Mooney-Rivlin methods.

	Swelling method	Mooney – Rivlin		
Samples	Crosslink density (mol/cc)	Slope (c_2)	Intercept (c_1)	Crosslink density (mol/cc)
N18	0.243 x 10^{-6}	0.1915	0.0277	0.112 x 10^{-6}
N26	6.48 x 10^{-6}	0.2232	0.0143	5.77 x 10^{-6}
N33	7.05 x 10^{-6}	0.2850	0.0165	6.64 x 10^{-6}
N44	8.28 x 10^{-6}	0.3323	0.0190	7.69 x 10^{-6}

[a] The sample from N49 was very brittle and the swelling experiment was not performed.

Dynamic mechanical properties of the NBR compounds were studied as a function of temperature. Fig. 8a–b showed the variation of storage modulus (E′) and loss tangent (tan δ) for the pure NBR (gum) and its crosslinked state. As expected, a gradual decrement of the storage modulus values at higher temperature indicated a flowing behavior for the uncrosslinked (pure) N18 sample, whereas, $ZnCl_2$ cured sample showed a rubbery plateau at higher temperature. It was also observed that crosslinked sample displayed higher storage modulus as compared to pure NBR. This behavior could be attributed to the crosslinked nature of the matrix imparted by $ZnCl_2$.

A couple of interesting observations were found from the loss tangent (tan δ) vs. temperature plots. The tan δ peak value of the vulcanizate significantly dropped down almost three times as compared to the raw rubber (Fig. 8b). Moreover, the position of the corresponding tan δ peak also significantly shifted towards higher temperature (−36.9 to −30.8 °C) for the crosslinked rubber. This tan δ peak is also unusually broadened with respect to temperature. These findings not only clearly revealed the high crosslinked density of NBR matrix, but also the polymer chains are relaxed with different dynamics along with cooperative movements of the α relaxation. At least some of the polymer chains have reduced mobility relative to the mobility of the bulk. This can be interpreted if we consider a srong interfacial interaction of the zinc-nitrle complex (Fig. 1b) with NBR chains which is immobilised as compared with the bulk. Surprisingly, apart from glass transition peak

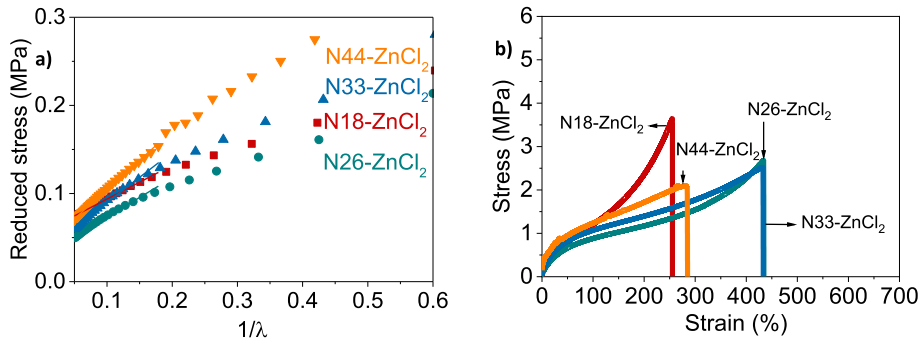

Fig. 7. a) Mooney-Rivlin plot for the NBR vulcanizates cured with $ZnCl_2$, b) the stress-strain plot of the crosslinked NBR vulcanized by $ZnCl_2$.

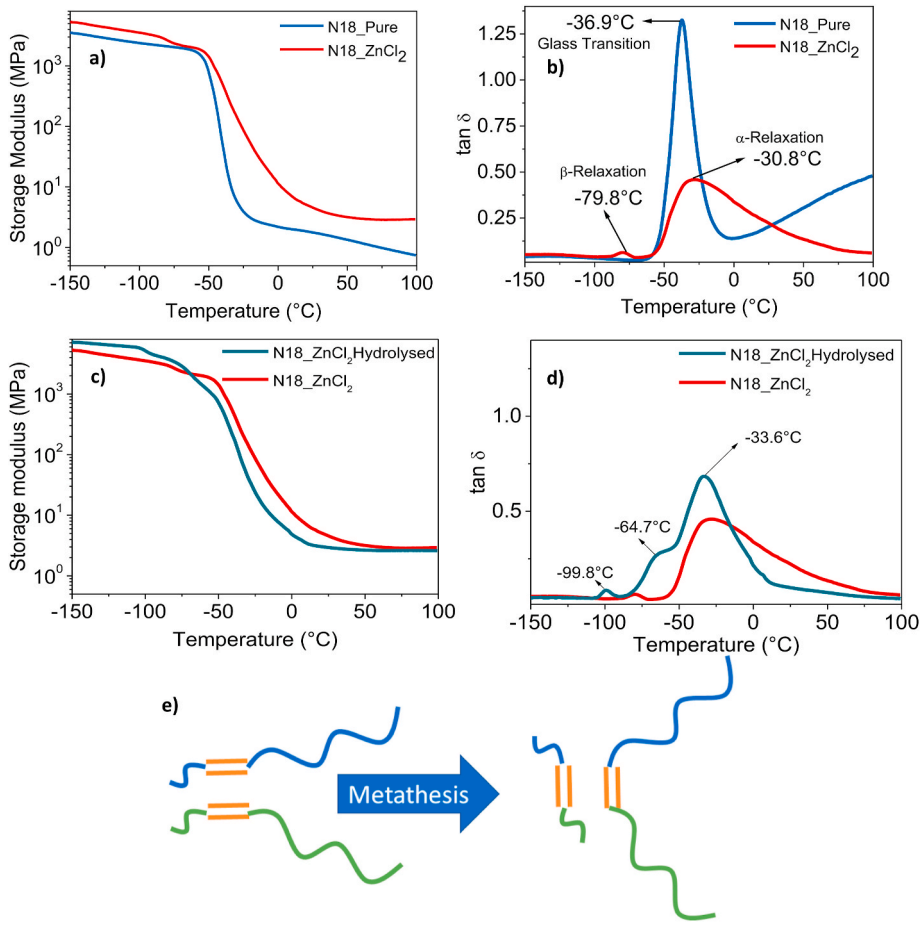

Fig. 8. Dynamic mechanical a) loss tangent, b) storage modulus as a function of temperature of the pure NBR and $ZnCl_2$ crosslinked NBR, c) loss tangent, d) storage modulus as a function of temperature of the $ZnCl_2$ crosslinked sample and the hydrolyzed sample which was previously crosslinked with $ZnCl_2$, e) probable scheme of exchange metathesis and evolution of fragmental chains catalyzed by acrylonitrile-Zn complex.

[39], another new peak appeared at relatively lower temperature at −79.8 °C [38–41]. The reason of appearance of such sub-T_g low temperature relaxation of NBR compound was still unknown but somehow also could be speculated with the metathesis type of reaction assisted by acrylonitrile $ZnCl_2$ complex [42,43]. Formation of small fragmental chain during metathesis as shown in Fig. 8e could be responsible for such low temperature behavior [44]. This behavior could be also associated with the non-cooperative motion of the fragmented portions or the dangling chains (produced during the crosslinking and metatheses) of the macromolecule. A detail study of such cross-metathesis reaction of NBR by $ZnCl_2$ is required to understand this phenomenon. However, this is beyond the scope of this article. To the best of authors' knowledge, the appearance of such low temperature relaxation, apart from the usual α-relaxation of NBR compound was not reported before.

Now, it would be interesting to discuss the dynamic mechanical spectra obtained from hydrolyzed sample. It could be clearly observed that the storage modulus of the hydrolyzed sample did exactly match with the un-hydrolyzed sample at rubbery plateau region indicting unaltered crosslink densities of both the samples.

Interestingly, in accordance to the DMA plot, the hydrolyzed crosslinked matrix showed additional two relaxation processes apart from the main glass transition of the polymer. The three such peaks appeared at −33.6 °C, −64.7 °C, −99.8 °C. The original sample ($ZnCl_2$ crosslinked) demonstrated the glass transition (T_g) −30.8 °C which further shifted to

−33.6 °C. The middle peak at −64.7 °C and the further low temperature peak at −99.8 °C corroborated to the other segmental non-cooperative relaxation of the hydrolyzed polymers [44]. It is already discussed that treatment of $ZnCl_2$, crosslinking at higher temperature and subsequent hydrolysis of the sample can generate various chemical functional groups as side chain like carboxylic, amide etc. These newly generated functional groups also could contribute these low temperature relaxations. Furthermore, the possibilities of the fragmentation of the macromolecular chain into shorter molecular weight by nitrile-zinc complex cannot be neglected. This low molecular weight NBR may have also lower glass transition and that is reflected in the tan δ vs. temperature curve.

The low-temperature relaxation process of crosslinked NBR was further substantiated from the DSC study. The corresponding DSC curves were exhibited in Fig. 9a–b. In this DSC study, the glass transition temperature of pure NBR was found to be at −48.6 °C with ΔC_p value of 0.562 J/gK. After crosslinking with $ZnCl_2$, this peak appeared to be shifted towards higher temperature to −44.5 °C with ΔC_p value of 0.311 J/gK. The shifting of T_g of the crosslinked sample to higher temperature as evinced from DSC study corroborated with the findings obtained from DMA results. Furthermore, the crosslinked sample also exhibited an extra transition at lower temperature (−87.9 °C) with a corresponding ΔC_p value of 0.094 J/gK which is much smaller ΔC_p values as compared with ΔC_p value of other transition value. The higher ΔC_p corresponds with the glass transition process which is resulting from the main chain relaxation (glass transition) and the lower ΔC_p is associated with the non-cooperative motion of the fragmented or dangling chains [45,46]. These facts were also evinced by DMA results discussed earlier.

Surprisingly, for hydrolyzed sample, unlike DMA findings, only two different thermal processes were witnessed in the DSC plot. One is the glass transition at −102.2 °C with very small ΔC_p value of 0.052 J/gK and the other is a very strong melting endotherm with a peak value of 10 °C (Fig. 9c). Zinc chloride could form six different hydrates with the general formula $ZnCl_2(H_2O)_n$ and the values of n was largely dependent on the hydration sheath [47]. Likewise, due to existence of polymorphic structure of hydrated $ZnCl_2$ the melting and crystallization behaviour is found to be taken place in a wide temperature window. It is obvious that the water crystallites formed within the structure of the hydrolyzed specimen had undergone melting at higher temperature. The disappearance of the glass transition temperature of the hydrolyzed specimen could be attributed to the melting of ice formed from the clustered water in the structure and therefore plasticizing effect of water was primarily responsible for suppressing the glassy transition [48–50]. Water-based cross-links tend to form, leading to increased water-water interactions at the expense of water-polymer chain interactions [51]. Henceforth, the absence of the crystallization peaks indicated that hydrophilic rubber could not crystalize or possibly merge with the water crystallization peak below room temperature. A mild transition at −102.2 °C which is attributed to the β-relaxation and this particular transition at low temperature did not alter its position and nature in the DSC plot if compared to the corresponding DMA plot. Fig. 9d showed the cooling curve of the hydrolyzed sample at a constant rate of cooling. The ice-melting endotherm at ∼ −60.6 °C on the DSC thermograms depicted in Fig. 9d resulted from the condensed water crystals in the hydrolyzed specimen [52–54]. The water crystals formed from water molecules had sufficient mobility for intermolecular interactions during rapid cooling (in this case 20K/min) in the DSC.

Crystallization being an exothermic process, heat is released to the surroundings resulting into a dip in the plot of heat flow versus temperature as demonstrated in Fig. 9d. The area under the curve as exhibited by blue checkered area corresponded to −84.88 J/gK, the latent heat of crystallization for the crystalline water of $ZnCl_2$.

The SEM micrograph of the N18 sample is displayed in Fig. 10a–c. $ZnCl_2$ was observed to be homogeneously distributed into the NBR matrix and did not generate any phase-separated morphology. The corresponding EDX spectra of the same sample, as demonstrated in Fig. 10b, evinced the elemental presence of zinc, chlorine and oxygen atoms on the surface. The mapping images produced through EDX

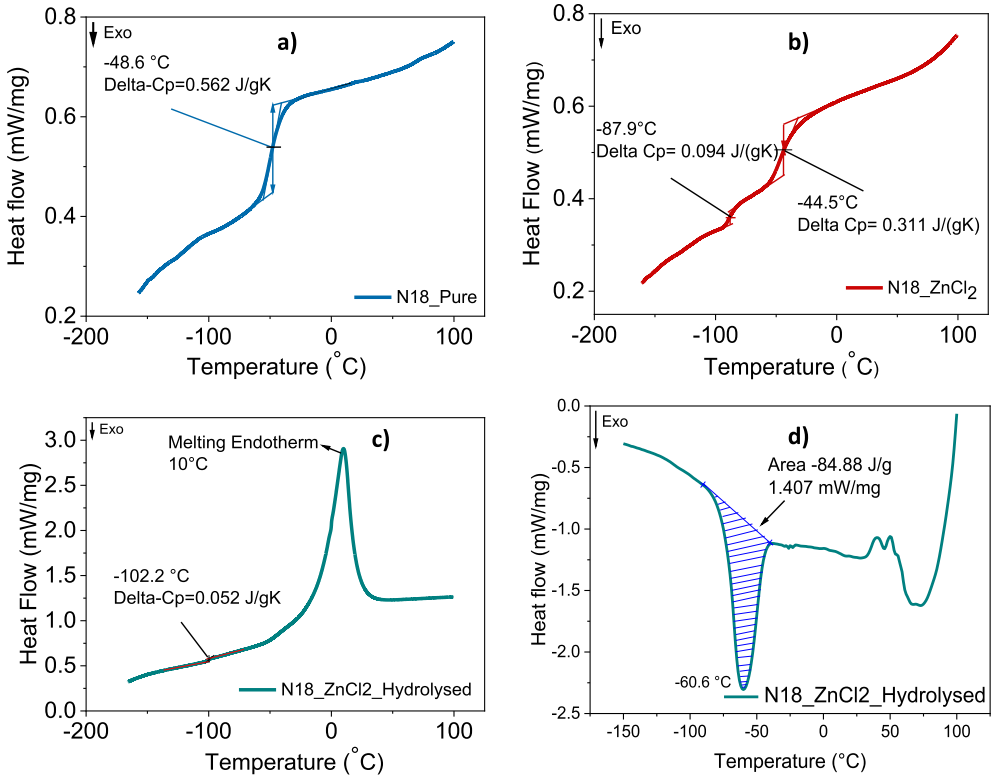

Fig. 9. Differential scanning calorimetry (DSC) curves of (a) raw rubber and (b) its vulcanizates, (c) melting endotherm curve (2nd heating) recorded in DSC and d) cooling curve at constant rate for hydrolyzed nitrile rubber compound.

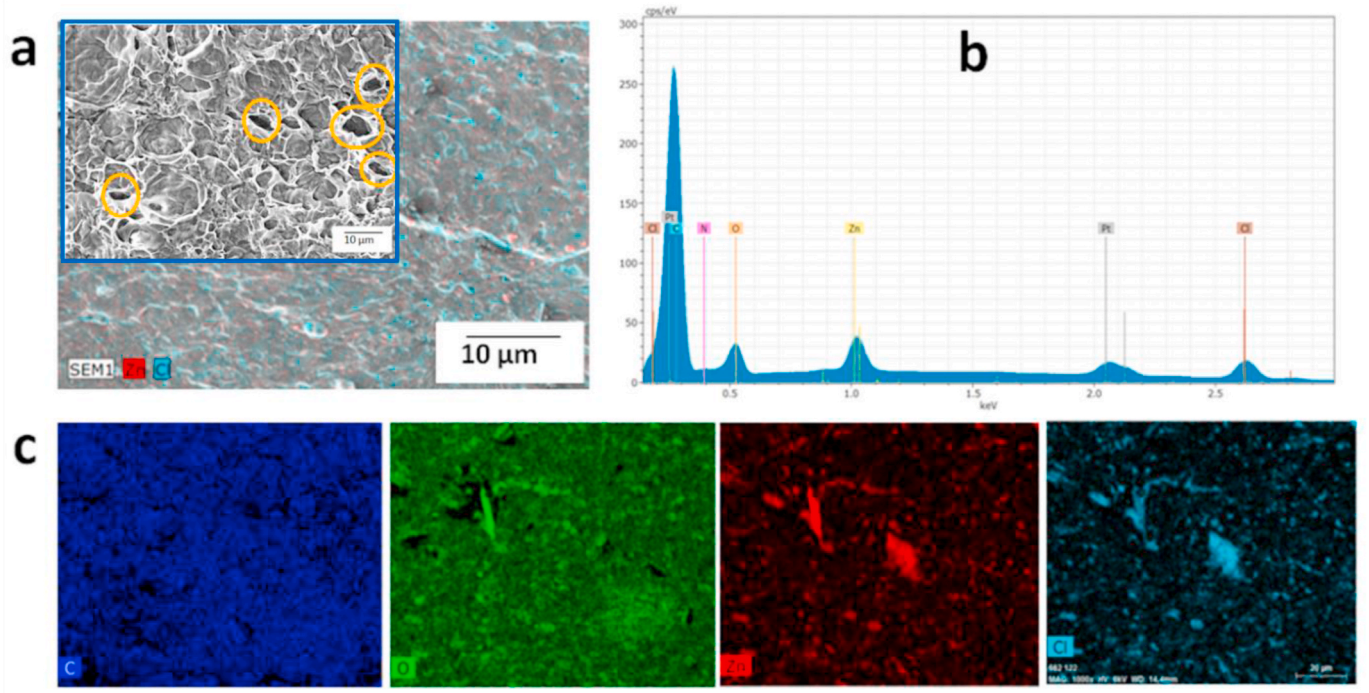

Fig. 10. (a) SEM micrograph, (b) EDX spectra and (c) carbon, oxygen, zinc and chlorine mapping of N18 sample. The peaks in EDX spectra corresponding to Pt originate from the sample holder (sputtering). Inset of Fig. 10a: SEM of hydrolyzed sample.

scanning exhibited how in the uniform carbonaceous matrix of NBR rubber, the elemental presence of zinc and chlorine atoms are dispersed to a fair extent.

Previous report [11], suggested that amount of $ZnCl_2$ mixed with nitrile rubber played a significant role to generate a specific type of microstructure in such compounds. 20 phr $ZnCl_2$ produced a 'macro--homogeneous' microstructure with the NBR matrix. However, some $ZnCl_2$ particles are found in the elemental mapping where oxygen, zinc and chlorine are spotted with bright appearance. The SEM micrograph of the hydrolyzed sample has generated more rough surfaces in the microstructure (Inset of Fig. 10a). Porous structure seems to be appeared in the whole area of the corresponding rubber specimen. The change in the microstructure in case of hydrolyzed sample with respect to the unhydrolyzed (Fig. 10a) one is pretty obvious.

5. Conclusions

The low-temperature relaxation behavior of NBR treated with $ZnCl_2$ was explored in this study. The possible microstructures of the cross-linked units of the zinc-nitrile complexes were schematically presented. Evolution of those chemical functional groups as well as the fragmentation of NBR with lower molecular weight polymer could be the reason of multi-relaxation processes which were found in DMA as well as in DSC studies. It is proposed that the nitrile groups are chemically interacting with $ZnCl_2$ and a zinc-nitrile complex could be formed; and in the next step this complex could generate a cross-metathesis type reaction resulting to low molecular weight polymers. Surprisingly, a triazine structure was found with commercially available NBR which was detected in the FTIR study. The microstructure was found to be changed after hydrolysis and porous structure was obtained as observed from SEM images. Additionally, proper care should be taken for the use of conventional rubber mixing equipment as large amount of $ZnCl_2$ could chemically react with the metal parts. Other characterization techniques like, e.g. dielectric spectroscopy, could be suitable tools for further studies of this interesting system.

Declaration of competing interest

The authors declare that they have no known competing financial interests or personal relationships that could have appeared to influence the work reported in this paper.

Acknowledgement

Some parts of the work were supported by the Priority Programme "Soft Material Robotic Systems" (SPP 2100) from Deutsche Forschungsgemeinschaft (DFG). The authors want to acknowledge the following people from Leibniz-Institut für Polymerforschung Dresden e. V.: Ms. Sabina Krause for the thermal analyses, Ms. M. Auf der Landwehr for the SEM-EDX, and S. Wießner, K.W. Stoeckelhuber for their fruitful discussions. We wish to also acknowledge the constructive and critical scientific discussion offered by Prof. Dr. Chayan Das, VNIT Nagpur.

References

[1] B. Slade, Elastomerics 117 (11) (1985) 34.
[2] G.L.M. Vroomen, G.W. Visser, J. Gehring, Electron beam curing of EPDM, Rubber World 205 (2) (1991) 23.
[3] B. Thorburn, Y. Hoshi, Rubber World 206 (4) (1992) 17.
[4] W. Hofmann, Rubber Technology Handbook, Hanser Publishers, Munich, Germany, 1989, p. 404.
[5] A.K. Bhowmick, D. Mangaraj, in: A.K. Bhowmick, M.M. Hall, H.A. Benary (Eds.), Rubber Products Manufacturing Technology, Marcel Dekker Inc., New York, 1994, p. 385.
[6] M. Myhre, D.A. MacKillop, Rubber recycling, Rubber Chem. Technol. 75 (2002) 429–474.
[7] L.M. Polgar, M. van Duin, A.A. Broekhuis, F. Picchioni, Use of diels–alder chemistry for thermoreversible cross-linking of rubbers: the next step toward recycling of rubber products? Macromolecules 48 (2015) 7096–7105.
[8] K. Chino, M. Ashiura, Themoreversible cross-linking rubber using supramolecular hydrogen-bonding networks, Macromolecules 34 (2001) 9201–9204.
[9] P. Cordier1, F. Tournilhac, C. Soulié-Ziakovic, L. Leibler, Self-healing and thermoreversible rubber from supramolecular assembly, Nature 451 (2008) 977–980.
[10] D. Montarnal, M. Capelot, F. Tournilhac, L. Leibler, Silica-like malleable materials from permanent organic networks, Science 334 (2011) 965–968.

[11] D. Basu, A. Das, K.W. Stöckelhuber, D. Jehnichen, P. Formanek, E. Sarlin, J. Vuorinen, G. Heinrich, Evidence for an in situ developed polymer phase in ionic elastomers, Macromolecules 47 (2014) 3436–3450.
[12] L. Ibarra, A. Rodríguez, I. Mora-Barrantes, Crosslinking of carboxylated nitrile rubber (XNBR) induced by coordination with anhydrous copper sulfate, Polym. Int. 58 (2009) 218–226.
[13] U.K. Mandal, D.K. Tripathy, S.K. De, Dynamic mechanical spectroscopic studies on plasticization of an ionic elastomer based on carboxylated nitrile rubber by ammonia, Polymer 37 (1996) 5739–5742.
[14] P. Antony, S.K. De, Ionic thermoplastic elastomers: a review, J. Macromol. Sci. Polym. Rev. 41 (1–2) (2001) 41–77.
[15] R. Rajeshbabu, U. Gohs, K. Naskar, M. Mondal, U. Wagenknecht, G. Heinrich, Electron-induced reactive processing of poly(propylene)/ethylene–octene copolymer blends: a novel route to prepare thermoplastic vulcanizates, Macromol. Mater. Eng. 297 (7) (2012) 659–669.
[16] S.S. Banerjee, A. Janke, U. Gohs, A. Fery, G. Heinrich, Some nanomechanical properties and degree of branching of electron beam modified polyamide 6, Eur. Polym. J. 88 (2017) 221–230.
[17] M. Mondal, U. Gohs, U. Wagenknecht, G. Heinrich, Polypropylene/Natural rubber thermoplastic vulcanizates by eco-friendly and sustainable electron induced reactive processing, Radiat. Phys. Chem. 88 (2013) 74–81.
[18] A. Erxleben, Structures and properties of Zn(II) coordination polymers, Coord. Chem. Rev. 246 (2003) 203–228.
[19] C. Shao, Y. Mao, P. Shang, Q. Li, C. Wu, Improved tensile strength of acrylonitrile–butadiene rubber/anhydrous copper sulfate composites prepared by coordination cross-linking, *Polym*, Bulletin 76 (2019) 1435–1452.
[20] F. Shen, H. Li, C. Wu, Crosslinking induced by in-situ coordination in acrylonitrile butadiene rubber/poly(vinyl chloride) alloy, filled with anhydrous copper sulfate particles, J. Polym. Sci., Polym. Phys. Ed. 44 (2) (2006) 378–386.
[21] N.D. Zakharov, Vulcanization of some synthetic rubbers without sulphur–IV. the effect of the nitrile-group content on the thermal vulcanization of butadiene-nitrile rubbers *Vysokomol*, Soyed 5 (8) (1963) 1190–1195.
[22] N.D. Zakharov, V.A. Kuznetsova, *Vysokomol. Soyed.* 5th report in the series ''Nonsulphur vulcanization of certain synthetic rubbers'' A10 (2) (1968) 331–338.
[23] S. Wu, S. Fang, Z. Tang, F. Liu, B. Guo, Bioinspired design of elastomeric vitrimers with sacrificial metal-ligand interactions leading to supramechanical robustness and retentive malleability, Mater. Des. 192 (2020) 108756.
[24] H. Mou, F. Shen, Q. Shi, Y. Liu, C. Wu, W. Guo, A novel nitrile butadiene rubber/zinc chloride composite: coordination reaction and miscibility, Eur. Polym. J. 48 (4) (2012) 857–865.
[25] J. Dechant, Ultrarotspektroskopische Untersuchungen an Polymeren, Akademie Verlag, Berlin, 1972.
[26] G. Socrates, in: Infrared and Raman Characteristic Group Frequencies: Tables and Charts, third ed., John Wiley & Sons, Ltd., Chichester, 2004.
[27] P.J. Flory, J. Rehner, Statistical mechanics of cross-linked polymer networks II. Swelling, J. Chem. Phys. 11 (1943) 512–521.
[28] Chapter 5 - Liquid Transport through Elastomers, Author Links Open Overlay Panel, Thomasukutty Jose, Soney C.George, Transport Properties of Polymeric Membranes, Elsevier, 2018, pp. 71–89.
[29] H. Desai, K.G. Hendrikse, C.D. Woolard, Vulcanization of polychloroprene rubber. I. A revised cationic mechanism for ZnO crosslinking, J. Appl. Polym. Sci. 105 (2007) 865–876.
[30] E.N. Zil'berman, The reactions of nitrile-containing polymers, 1986, Russ. Chem. Rev. 55 (1) (1986) 62–78. Translated from Uspekhi Khimii, 55.
[31] T.L. Cairns, A.W. Larchar, B.C. McKusick, The trimerization of nitriles at high pressures, J. Am. Chem. Soc. 74 (22) (1952) 5633–5636.
[32] Shiwei Liu, Shuang Tan, Bing Bian, Hailong Yu, Qiong Wu, Zhiguo Liu, Fengli Yu, Li Lu, Shitao Yu, Xiuyan songc and zhanqian songa, isobutane/2-butene alkylation catalyzed by brønsted–lewis acidic ionic liquids, RSC Adv. 8 (2018) 19551–19559.
[33] V. M. Litvinov and P. P. De Spectroscopy Of Rubbers and Rubbery Materials, Shropshire, Rapra Technology Ltd, UK, P. 113.
[34] M. Imoto, T. Otsu, M. Nakabayashi, Vinyl polymerization. LXIX. The polymerization of a complex of acrylonitrile with zinc chloride, Makromol. Chem. 65 (1963) 194–201.
[35] G. Socrates, in: Infrared and Raman Characteristic Group Frequencies, third ed., John Wiley & Sons Ltd., 2004, p. 130.
[36] J. Furukawa, Y. Onouchi, S. Inagaki, H. Okamoto, Rubber elasticity at very large elongation, Polym. Bull. 6 (1982) 381–387.
[37] R. Hagen, L. Salmén, B. Stenberg, Effects of the type of crosslink on viscoelastic properties of natural rubber, J. Polym. Sci. B Polym. Phys. 34 (1996) 1997–2006.
[38] A.D. Roberts, Natural Rubber Science and Technology, Oxford University Press, Oxford, UK, 1988 xvii + 1136.
[39] M. Makrocka-Rydzyk, G. Nowaczyk, S. Głowinkowski, S. Jurga, Dynamic mechanical study of molecular dynamics in ethylene–norbornene copolymers, Polymer 51 (2010) 908–912.
[40] T. Pakula, A Model of cooperative motions in dense polymer systems by means of closed dynamic loops in *Permanent and Transient Networks*, Prog. Colloid Polym. Sci. 75 (1987) 171–178.
[41] S. Yagihara, K. Hikichi, Cooperative interaction on side-chain motion of poly (α-amino acid), Polym. J. 14 (1982) 233–240.
[42] K. Saalwächter, A heuer, chain dynamics in elastomers as investigated by proton multiple-quantum NMR, Macromolecules 39 (2006) 3291–3303.
[43] R.F. Smith, S.C. Boothroyd, R.L. Thompson, E. Khosravi, A facile route for rubber breakdown via cross metathesis reactions, Green Chem. 18 (2016) 3448.
[44] H.Y. Mou, Y.Y. Cao, F. Shen, X.F. Yuan, C.F. Wu, Study on the non-liquid-phase coordination crosslinking reaction of acrylonitrile-butadiene rubber/copper sulfate composites, Acta Polym. Sin. 9 (2008) 910–913.
[45] A.G. Clark, M. Salcedo Montero, N.D. Govinna, S.J. Lounder, A. Asatekin, P. Cebe, Relaxation dynamics of blends of PVDF and zwitterionic copolymer by dielectric relaxation spectroscopy, J. Polym. Sci. 58 (9) (2020) 1311–1324.
[46] Z.Y. Cheng, S. Gross, J. Su, Q.M. Zhang, Pressure-temperature study of dielectric relaxation of a polyurethane elastomer, J. Polym. Sci. B Polym. Phys. 37 (10) (1999) 983–990.
[47] J. Braunstein, Solution chemistry in liquid mixtures of inorganic salts with water, Inorg. Chim. Acta. 2 (1968) 19–30, https://doi.org/10.1016/0073-8085(68)80012-9.
[48] Y.N. Zil'berman, R. Sh Frenkel', N.B. Vorontsova, N.A. Pitkevich, E.A. Kuz'mina, Mechanism of vulcanization of butadine-nitrile rubber by zinc chloride, Polym. Sci. 15 (1973) 1288–1291.
[49] M.Y.M. Chiang, M. Fernandez-Garcia, Relation of swelling and T_g depression to the apparent free volume of a particle-filled, epoxy-based adhesive, J. Appl. Polym. Sci. 87 (2003) 1436–1444.
[50] R.J. Young, P.A. Lovell, An Introduction to Polymers, Chapman & Hall, London, 1991.
[51] D. Steinerová, A. Kalendová, J. Machotová, M. Pejchalová, Environmentally friendly water-based self-crosslinking acrylate dispersion containing magnesium nanoparticles and their films exhibiting antimicrobial properties, Coatings 10 (4) (2020) 340.
[52] G.E. Schaumann, E.J. LeBoeuf, Glass transitions in Peat: their relevance and the impact of water, Environ. Sci. Technol. 39 (2005) 800–806.
[53] G. Pairoh, T. Tipvarakarnkoon, Thermal analysis of lipid crystallization and water ice on coconut milk emulsions: effect of NaCl concentrations, J. Med. Bioeng. 2 (3) (2013) 191–195.
[54] J.E. House, C.D. Dunbar, A DSC study of the phase transitions in $(CH_3)_3NH[CdCl_3]$, Thermochim. Acta 204 (1992) 213–219.